Photochemical & Photobiological Sciences

Accepted Manuscript

This is an *Accepted Manuscript*, which has been through the Royal Society of Chemistry peer review process and has been accepted for publication.

Accepted Manuscripts are published online shortly after acceptance, before technical editing, formatting and proof reading. Using this free service, authors can make their results available to the community, in citable form, before we publish the edited article. We will replace this *Accepted Manuscript* with the edited and formatted *Advance Article* as soon as it is available.

You can find more information about *Accepted Manuscripts* in the Information for Authors.

Please note that technical editing may introduce minor changes to the text and/or graphics, which may alter content. The journal's standard Terms & Conditions and the Ethical guidelines still apply. In no event shall the Royal Society of Chemistry be held responsible for any errors or omissions in this *Accepted Manuscript* or any consequences arising from the use of any information it contains.

ROYAL SOCIETY OF CHEMISTRY

www.rsc.org/pps

Photochemical transformation of iron(III)–arsenite complex in acidic aqueous solution

Ivan P. Pozdnyakov[*b],‡ Wei Ding[a],‡ Jing Xu[a], Long Chen[a,c], Feng Wu[*a], Vjacheslav P. Grivin[b], Victor F. Plyusnin[b]

[a] *Department of Environmental Science, Wuhan University, 430072 Wuhan, Hubei, P. R. China.*
[b] *Voevodsky Institute of Chemical Kinetics and Combustion, Institutskaya str. 3, 630090 Novosibirsk, Russian Federation, Novosibirsk State University, Pirogova str. 2, 630090, Novosibirsk, Russian Federation*
[c] *Department of Chemical and Environmental Engineering, University of California, Riverside, Riverside, California, 92521, US.*

*Corresponding authors:

Feng Wu, professor. Department of Environmental Science, Wuhan University, 430072 Wuhan, Hubei, P. R. China. Tel: +86(27)68778511, Fax: 86-27-68778511, E-mail: fengwu@whu.edu.cn.

Ivan P. Pozdnyakov, Dr. Voevodsky Institute of Chemical Kinetics and Combustion, Institutskaya str. 3, 630090 Novosibirsk, Russian Federation, Novosibirsk State University, Pirogova str. 2, 630090, Novosibirsk, Russian Federation. E-mail: pozdnyak@kinetics.nsc.ru.

‡ These authors contributed equally to this work.

Abstract

Surface complexation between arsenious acid anions (As(III)) and ferric (hydr)oxides in water is important for the transformation and transfer of inorganic arsenic species. The mechanisms of formation and the photochemistry of dissolved Fe(III)–As(III) complexes in acidic aqueous solution are still unclear. Here, the photooxidation of As(III) in the presence of Fe(III) ions in acidic media has been investigated by laser flash and steady-state photolysis. At low arsenite concentration (< 1 mM), As(III) is oxidized by $^{\bullet}OH$ radical generated by photolysis of the $FeOH^{2+}$ complex. At higher arsenite concentrations (>10 mM), photoactive Fe(III)–As(III) complexes are formed ($\phi_{Fe}^{308} \approx 0.012$). At all arsenite concentrations, white $FeAsO_4$ colloid is formed during As(III) photolysis in the presence of Fe(III) ions. Solid Fe(III)–As(III) complexes have been prepared and characterized, and the photochemical transformation of As(III) to As(V) in solid Fe(III)–As(III) complexes has been confirmed. These findings are important for a better understanding of the evolution of As(III) species under environmental conditions and should provide guidance for detoxification of As(III)-polluted water systems.

***Keywords*:** Arsenite, arsenate, iron complexes; laser flash photolysis; $^{\bullet}OH$ radical; photooxidation

Introduction

The problem of arsenic contamination requires urgent attention on a global scale because of its carcinogenicity and toxicity. Thus, there has been great scientific interest in the chemistry and transformation of arsenic species in the environment.[1–3] In natural waters, arsenic exists in two main inorganic forms: arsenite in the form of $H_3As(III)O_3$ and arsenate in the form of $H_2As(V)O_4^-$ and $HAs(V)O_4^{2-}$. In an investigation of 65 well water samples in the United States, Sorg et al.[4] found that arsenic existed mainly as As(V) in 31 wells, mainly as As(III) in 29 wells, and as a mixture in the remaining 5 wells. The occurrence of

arsenic species is affected by environmental conditions. In particular, photochemical reactions under ultraviolet (UV) and visible light may lead to the oxidation of arsenite to arsenate.[5–7]

In previous studies, the effects of dissolved ions and (hydr)oxides of transition metals (especially iron) have been extensively examined. These species were found to play an important role in co-precipitation/adsorption[2,8,9] and in (photo)catalytic oxidation of As(III) to As(V) by dissolved oxygen and hydrogen peroxide[10–13]. As(III) photooxidation on the surface of different kinds of (hydr)oxides (ferrihydrite[14], goethite[15,16], montmorillonite[17], etc.) has raised concerns in this decade. However, previous studies have been mainly concerned with the generation of reactive oxygen species (ROS); the relationship between Fe and As, including photooxidation mechanisms of As(III), has usually been beyond the scope of such studies. In recent years, the concept of complexation between arsenic and iron (hydr)oxides has been proposed, and related works have been published in this area.[14,16,18] Although such works have revealed the ability of arsenic to complex with iron (hydr)oxides, the corresponding oxidation mechanisms were still unclear until early 2014. Xu et al.[19] proposed a novel pathway involving ligand-to-metal charge transfer (LMCT) for arsenic oxidation in colloidal ferric hydroxide (CFH) systems. Their work confirmed the complexation between As(III) and CFH and they elucidated the complex formation equilibrium constants at near-neutral pH (6.0). However, in this study, the possibility of complexation between As(III) and free Fe(III) ions in aqueous solution was not considered, and the photochemical reaction of the Fe(III)–As(III) complex in aqueous solution remains unclear. To obtain a dissolved Fe(III)–As(III) complex in aqueous media, the solution must be strongly acidic to prevent the formation of CFH.

The formation of As(IV) species as key intermediates is postulated in the ROS and LMCT mechanisms. However, the conclusion of As(IV) formation has been based mainly on indirect results of the determination of As(V) as the final oxidation product[20–22] or on the effect of different ROS scavengers on the As(III)

oxidation rate[13,16,19]. Direct spectral or kinetic observations of As(IV) species formation during As(III) photooxidation in the presence of iron complexes or (hydr)oxides are not yet available in the literature.

In the present work, optical spectroscopy, as well as steady-state (308 nm, XeCl excilamp) and nanosecond laser flash photolysis (LFP; 266 nm, 6 ns, Nd:YAG laser) have been used to study complexation and mechanistic aspects of the aqueous photochemistry of As(III) in the presence of Fe(III) in acidic media (pH 3). Attention has been mainly paid to the determination of active intermediates, the rate constants of elementary stages, as well as the construction of a detailed kinetic scheme for As(III) photooxidation in the presence of iron species. This information should prove very useful in understanding the oxidation of As(III) to As(V) in discharges of acid mine drainage (AMD), which contain high concentrations of both iron and arsenite.[23] The As(III) concentration used in this work was higher than that usually found in AMD to obtain good yields of Fe(III)–As(III) complexes, and experiments were conducted at low pH in order to prevent Fe(III) precipitation. Preliminary preparation, characterization, and photolysis experiments on the solid Fe(III)–As(III) complex were also conducted to demonstrate its photochemical activity in the solid state.

Experimental

Chemicals

All chemicals were of analytical grade and were used without further purification. As(V), As(III), and Fe(III) solutions in deionized water were prepared from Na_2HAsO_4 $7H_2O$ (Alfa Aesar, A Johnson Matthey Co., Tianjin, China), $NaAsO_2$ (Xiya Reagent Center, Sichuang, China), and $Fe(ClO_4)_3$ (Internet Aladdin Reagent Database Inc., Shanghai, China), respectively. Ethanol was purchased from Tianjin Kermel Chemical Reagent Co. Ltd. (Tianjin, China). Potassium borohydride (KBH_4), thiourea, ascorbic acid (VC), potassium hydroxide (KOH), sodium hydroxide (NaOH), hydrochloric acid (HCl), ammonium fluoride (NH_4F), acetic

acid (CH_3COOH), and *o*-phenanthroline (phen) were purchased from Sinopharm Chemical Reagent Co. Ltd. (Shanghai, China). Water of 18 MΩ cm resistivity was purified through a water purification system (Liyuan Electric Instrument Co., Beijing, China) and was used for preparation of all samples.

Preparation of solid Fe(III)–As(III) or Fe(III)–As(V) complex

Experiments were conducted by using 100 mL aqueous suspensions or solutions of analytical grade chemicals in a 250 mL beaker agitated mechanically by a magnetic stirrer. The reaction solution temperature was kept at 0 ℃ by using a low-temperature cooling-liquid circulating pump.

Reaction solutions were prepared in aqueous HCl (pH 1) with fixed concentrations of As(III) (354 mM), As(V) (118 mM), and Fe(III) (590 mM).

Preparation of Fe(III)–As(III) complex: 10 mL of Fe(III) reaction solution was added to 50 mL of As(III) reaction solution (Fe(III)/As(III) molar ratio 1:3) at a rate of about 500 μL/min, and then the solution was diluted to 100 mL and adjusted to pH 1. The solution was stirred for a further 2 h, whereupon 80–150 mL of absolute ethanol was added. The excess of As(III) was precipitated as As_2O_3 and the residue was separated from the supernatant by centrifugation at 10,000 rpm for 15 min. The Fe(III)–As(III) complex was collected by vacuum freeze-drying and washed with pure ethanol, retaining the supernatant. It was subsequently vacuum freeze-dried once more.

Preparation of Fe(III)–As(V) complex: 50 mL of As(V) reaction solution was added to 30 mL of Fe(III) reaction solution (Fe(III)/As(V) molar ratio 3:1) at a rate of ca. 2.5 mL/min, and then the solution was diluted to 100 mL and adjusted to pH 1. The solution was stirred for a further 2 h. The resulting suspension was centrifuged at 10,000 rpm for 15 min, and the precipitate was washed three times with aqueous HCl (pH 1). The product was dried at 60.0 ℃ for 6 h.

Photolysis equipment and analysis

The LFP setup in the time-resolved experiments was based on an LS-2137U Nd:YAG laser (Lotis TII, Belarus) with an excitation wavelength of 266 nm, a pulse duration of 5–6 ns, an illumination spot area of 0.03 cm^2 and an energy per pulse of up to 10 mJ. The device was similar to that described in a previous work.[24] The time resolution of the setup was ca. 50 ns. Solutions in LFP experiments were refreshed after each 100–150 pulses to avoid any possible influence of photogenerated $FeAsO_4$ flakes on the measurements. For steady-state irradiation in aqueous solutions, XeCl excimer lamps (308 nm, produced by the Institute of High Current Electronics, Tomsk, Russia) and the fourth harmonic of the Nd:YAG laser (266 nm) were used. The lamp and laser intensities were determined by means of a ferrioxalate actinometer.[25]

Unless otherwise specified, all photochemical experiments were performed in a 1 cm quartz cell in air-equilibrated or argon-saturated solutions at an initial pH≈3, at 298 K, and under atmospheric pressure. Argon-saturated solutions were obtained by constantly bubbling argon through the sample. UV spectra were recorded on an Agilent 8453 spectrophotometer (Agilent Technologies). pH measurements were carried out by using an ANION-4100 pH meter (Smolensk, Russia) with a combined electrode (ESK-10614).

Stability constants and absorption coefficients of the Fe(III)–As(III) complexes were estimated by numerical fitting of the optical density change at 260 nm using a subprogram (script) generated in-house with the commercially available Origin 8.0 software program and based on application of Newton's iterative optimization method[26] (see ESI (E-Supporting Information) section "Determination of stability constants and absorption coefficients of Fe(III)–As(III) complexes" for details).

The Fe(II) concentration after various photolysis times was measured by addition of the chelating agent o-phenanthroline to the irradiated solution and then measuring the absorption of the $[Fe(II)(phen)_3]^{2+}$ complex at 510 nm (the molar absorption coefficient at 510 nm is 11000 M^{-1} cm^{-1}).[25] To determine the total iron concentration, VC was added to reduce Fe(III) to Fe(II). The total iron concentration was then

determined in the same way as the Fe(II) concentration. The Fe(III) concentration was evaluated by a subtraction method.

Arsenic speciation was analyzed by means of hydride generation–atomic fluorescence spectrometry (HG–AFS; Titan Instruments Co. Ltd., Beijing, China). As(III) and total arsenic concentrations were determined by controlling the concentrations of HCl and KBH_4 during hydride generation, as conducted in our previous work.[27]

X-ray diffractograms were recorded on an X'Pert Pro X-ray diffractometer (Cu-$K_{\alpha 1}$ radiation, $\lambda = 1.54$ Å) operated at 40 kV and 40 mA. Scans were performed from 10 ° to 80 ° at a step size of 0.026 °. X-ray photoelectron spectroscopy (XPS) measurements were conducted on an ESCALAB 250Xi spectrometer using a monochromated Al-K_α X-ray source. A pass energy of 20 eV with a 0.050 eV step size was used for all samples. The XPS results were collected in binding energy form and were fitted by using a nonlinear least-squares curve-fitting program (XPS Peak 4.1). The XPS spectra were analyzed after subtracting the Shirley background applicable for transition metals. The percentage Lorentzian–Gaussian for fitting the data was set at 20%.

To demonstrate the photoactivity of the Fe(III)–As(III) complex in the solid state, steady-state photolysis of the solid product was performed. The solid Fe(III)–As(III) complex was the same batch as used in the XPS and XRD measurements and had an Fe/As molar ratio of 1:0.92. The sample was placed on filter paper under UV-C illumination (dominant wavelength 254 nm). The lamp (8 W, Cnlight Co., China) was fixed directly above the sample at a distance of 50 mm. The UV irradiation intensity on the surface of the sample was 2.0 W/m^2. The filter paper was divided equally into 16 parts. At each sampling time, the sample on one part of the filter paper was dissolved in 50 mL of $HClO_4$ solution at pH 1 for further measurement of arsenic species by HG–AFS.

Results and discussion

Formation of the Fe(III)–As(III) complexes in aqueous solution

The UV spectrum of the solution without As(III) was determined by the absorption of Fe^{3+} (λ_{max} = 240 nm; ε_{max} = 3800 M^{-1} cm^{-1}) and the $FeOH^{2+}$ complex (λ_{max} = 300 nm, ε_{max} = 1985 M^{-1} cm^{-1}).[28] The addition of arsenite ions (1–15 mM) at pH 3 led to an increase in UV absorption with a gradual shift of the absorption maximum from 300 to around 270 nm without appearance of any isosbestic points. These observations indicated complexation between As(III) and Fe(III) and the formation of more than one complex in solution (Fig. 1). Information on complexation between As(III) and Fe(III) is absent in the literature, but it is known that Fe(III) forms both 1:1 and 1:2 complexes with H_3PO_4[29] and H_3PO_3[30] in acid media. Hence, the following main equilibria in a solution containing $NaAsO_2$ and $Fe(ClO_4)_3$ at pH 3 should be taken into account:

$$NaAsO_2 + H_2O \rightleftharpoons Na^+ + H_2AsO_3^- \quad (1)$$

$$H_3AsO_3 \rightleftharpoons H_2AsO_3^- + H^+, \; pK_a = 9.2 \; [30] \quad (2)$$

$$Fe^{3+} + H_2O \rightleftharpoons FeOH^{2+} + H^+, \; pK_g = 2.2 \; [31] \quad (3)$$

$$Fe^{3+} + H_3AsO_3 \rightleftharpoons [Fe(H_2AsO_3)]^{2+} + H^+, \; pK_1 \quad (4)$$

$$[Fe(H_2AsO_3)]^{2+} + H_3AsO_3 \rightleftharpoons [Fe(H_2AsO_3)_2]^{+} + H^+, \; pK_2 \quad (5)$$

where K_a is the acid dissociation constant for H_3AsO_3, K_g is the hydrolysis constant of Fe^{3+}, and K_1,and K_2 are the stability constants of 1:1 and 1:2 Fe(III)–As(III) complexes. Here, it is assumed that Fe(III) forms complexes with $H_2AsO_3^-$ ion similarly to complexation with $H_2PO_3^-$.[30] The stability constants (pK_1, pK_2) and absorption coefficients (ε_1, ε_2) of the 1:1 and 1:2 Fe(III)–As(III) complexes were estimated by numerical fitting of a curve of the optical density change at 260 nm using Newton's iterative optimization method[26] (see ESI section "Determination of stability constants and absorption coefficients of Fe(III)-As(III) complexes" for details). The best fit gave pK_1 = 2.8, pK_2 = 2.5, ε_1 = 3 × 10^3 M^{-1} cm^{-1}, ε_2 = 4.3 × 10^3 M^{-1} cm^{-1}

corresponding to the predominant formation of a 1:2 complex $[Fe(H_2AsO_3)_2]^+$ (73% of total [Fe(III)]) at an As(III) concentration of about 1.5×10^{-2} M. We assumed that at arsenite concentrations >10 mM, the main photoactive species in solution would be the $[Fe(H_2AsO_3)_2]^+$ complex.

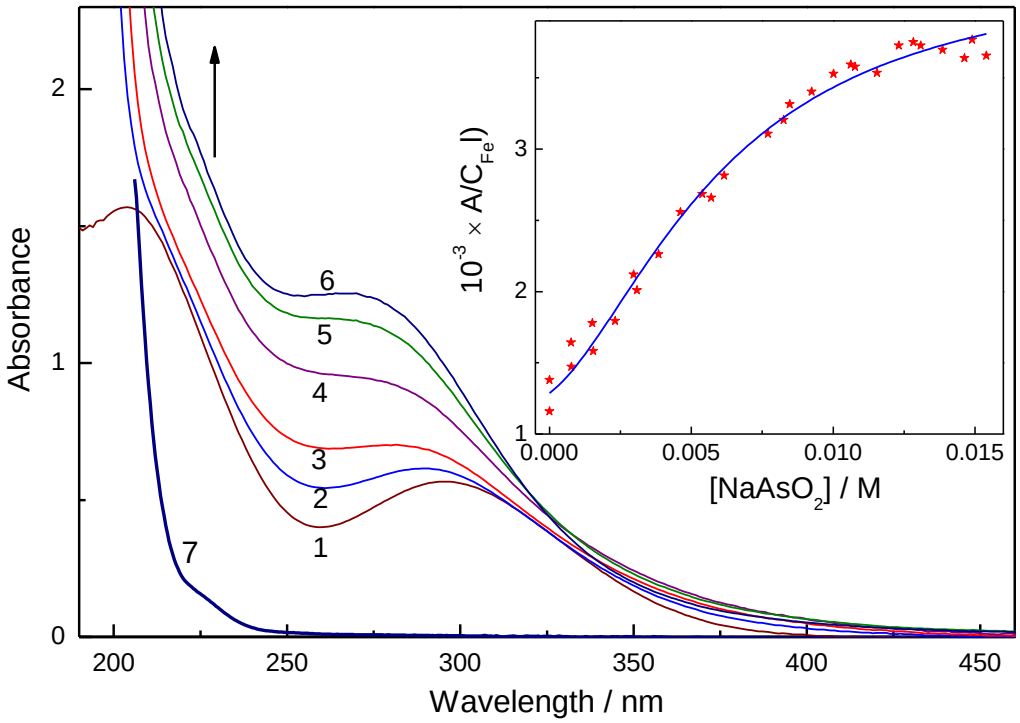

Fig. 1 Optical spectra of Fe(III) ions in the presence of 0 (1), 1.5 (2), 3.1 (3), 6.2 (4), 9.2 (5), and 15 mM (6) $NaAsO_2$. $[Fe(III)(ClO_4)_3]$ = 0.34 mM, pH 3. (7) Absorption spectrum of 15 mM $NaAsO_2$ alone. Inset: changes in optical density at 260 nm with the variation of $[NaAsO_2]$. The smooth curve is the best fit obtained by using Eq. (13) in the ESI.

Formation of the Fe(III)–As(III) complexes in the solid state

A solid Fe(III)–As(III) product was also prepared and characterized. The solid Fe(III)–As(III) product obtained by the procedure described in the Experimental Section was dissolved in aqueous $HClO_4$ at pH 1. The As(III) and Fe(III) concentrations in solution were measured by HG–AFS and spectrophotometry, respectively. The results indicated that the solid Fe(III)–As(III) product consisted of 11.68% As(III) and

192 6.23% Fe(III). No As(V) was observed. Considering the characteristic XRD bands of ferric arsenate at 2θ ≈
193 28° and 58°,[32] the sample was analyzed by XRD to identify its phase (Fig. 2). As the characteristic peaks of
194 the Fe(III)–As(III) complex were not apparent, it was concluded that this product chiefly consisted of an
195 amorphous phase.

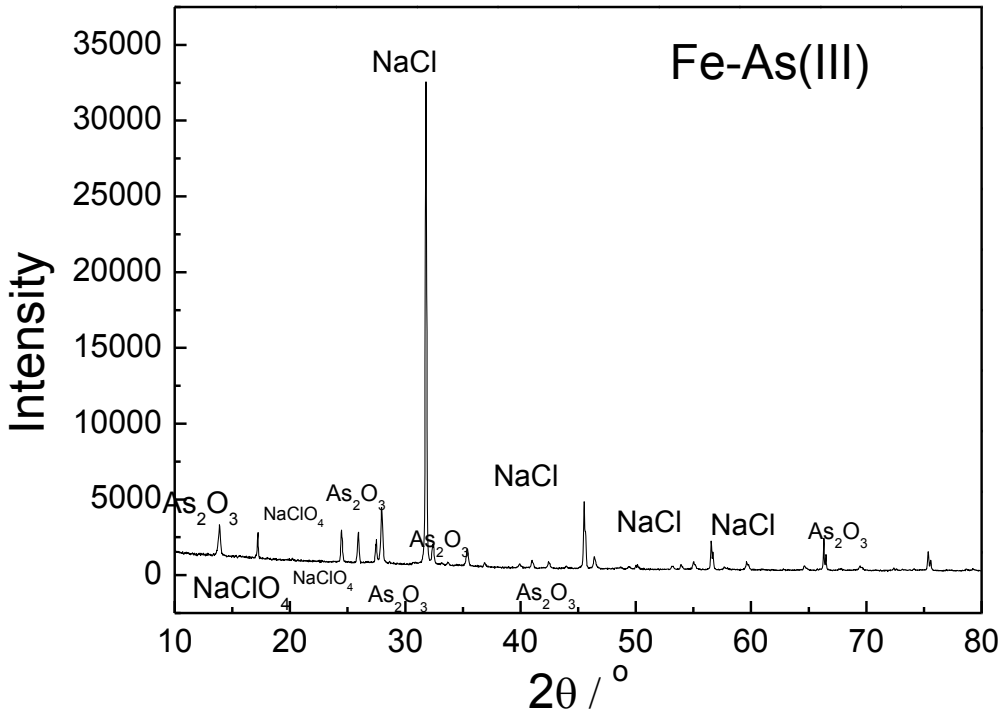

196

197 **Fig. 2** XRD pattern of solid Fe(III)–As(III) complex formed by direct mixing of Fe(III) and As(III) at pH 1
198 with ethanol. Experimental conditions: [Fe(III)(ClO_4)$_3$] = 59 mM, [As(III)] = 177 mM.

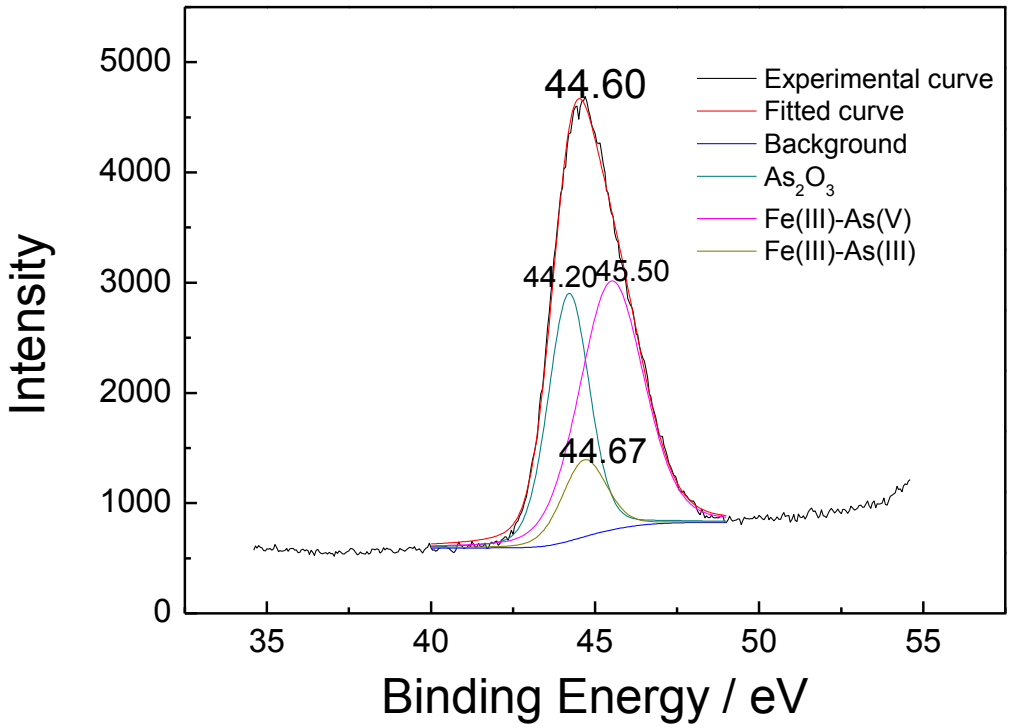

Fig. 3 As 3d XPS spectrum of solid Fe(III)–As(III) complex formed by direct mixing of Fe(III) and As(III) at pH 1 with ethanol. Experimental conditions: [Fe(III)(ClO_4)$_3$] = 59 mM, [As(III)] = 177 mM.

To verify the presence of arsenic and to determine the oxidation of As(III) on the solid surface of the Fe(III)–As(III) complex, the XPS spectrum of the solid Fe(III)–As(III) complex product was determined. The results in Fig. 3 analyzed by XPS Peak 4.1 indicated that the As 3d spectrum could be fitted by three species with binding energies at 44.20, 44.67, and 45.50 eV, respectively. The values of 44.20 and 45.50 eV can be attributed to As_2O_3[33] and As(V)[34], respectively.

In order to determine the form of As(V) (45.50 eV) in Fig 3, the As 3d XPS spectrum of the precipitate of the Fe(III)–As(V) complex formed by direct mixing of Fe(III) and As(V) at pH 1 was obtained (Fig. S1). This solid Fe(III)–As(V) complex was further dissolved to determine the ratio of Fe(III)/As(V). In this way, we confirmed that the Fe(III)–As(V) complex existed as $FeAsO_4$ with an approximately 1:1 Fe(III)/As(V) ratio. The position of the peak in Fig. S1 is the same as that in Fig. 3, that is, located at 45.50 eV, higher than

the binding energy of Na_3AsO_4 (44.9 eV).[35] Thus, the peak at 45.5 eV may be attributed to the higher binding energy for As(V)–O coordination to an iron atom, i.e., As(V)–O–Fe(III).[36]

However, the binding energy of As(III)–O is lower, at 44.6 ±0.13 eV;[36] thus, the peak at 44.67 eV can be assigned to As(III)–O–Fe(III). As shown in Fig. 3, As(III)–O–Fe(III) could be transformed to As(V)–O–Fe(III) due to oxidation of As(III) by the high-energy X-rays deployed during the measurement.[37] The XPS spectra in Figs. S2 and S3 suggest that Fe(II)–As complexation took place and that As(III)–O–Fe(III) was formed and underwent oxidation by X-ray energy. O_2 easily oxidized the generated Fe(II) under acidic conditions, resulting in a low Fe(II) concentration. As shown in Table S1, considering the data obtained from area estimation of the XPS spectra in Fig. 3 and the concentrations of arsenic species and iron species measured by HG–AFS and spectrophotometry, the amount of arsenic coordinated to iron was around 7.65%. Therefore, the Fe/As molar ratio of the solid complex was 1:0.92. However, the Fe/As ratio of the solid Fe(III)–As(III) complex differed from that of the dissolved Fe(III)–As(III) (1:2) complex estimated from UV spectrophotometric data (Fig. 1). Because the formation conditions of the complex were different, the compositions of the complex in solution and in the solid state were also different.

Photochemistry of the aqueous Fe(III)-As(III) system at high As(III) concentration: $[Fe(H_2AsO_3)_2]^+$ complex photolysis and As(IV) formation

Steady-state (308 nm) photolysis of the $[Fe(H_2AsO_3)_2]^+$ complex led to a disappearance of its absorption bands and the appearance of Fe(II) with a quantum yield of 0.012 (Fig. S4). The formation of white flakes was also observed during prolonged (ca. 60 min) steady-state irradiation at 308 nm at an incident light intensity of 1.4×10^{16} quanta/s or 0.56 mM/min, which indicated the generation of colloidal ferric arsenate ($FeAsO_4$) and occurrence of the reduction–oxidation reaction upon complex excitation. Similar results were obtained during irradiation of the $[Fe(III)(H_2AsO_3)_2]^+$ complex solution by pulses from an Nd:YAG laser at

266 nm. Decay of the complex absorption was observed with simultaneous Fe(II) photoproduction (the quantum yield of Fe(II) was estimated as 0.033). An increase in Fe(II) quantum yield with decreasing irradiation wavelength is a common feature of Fe(III) complex photochemistry.[38] The quantum yield of Fe(II) production from the $[Fe(H_2AsO_3)_2]^+$ complex was lower than those for $Fe(III)OH^{2+}$ or Fe_{aq}^{3+} (ϕ_{280} = 0.31 and 0.05, respectively) and comparable with that for $Fe(III)SO_4^+$ (ϕ_{280} = 0.008).[28]

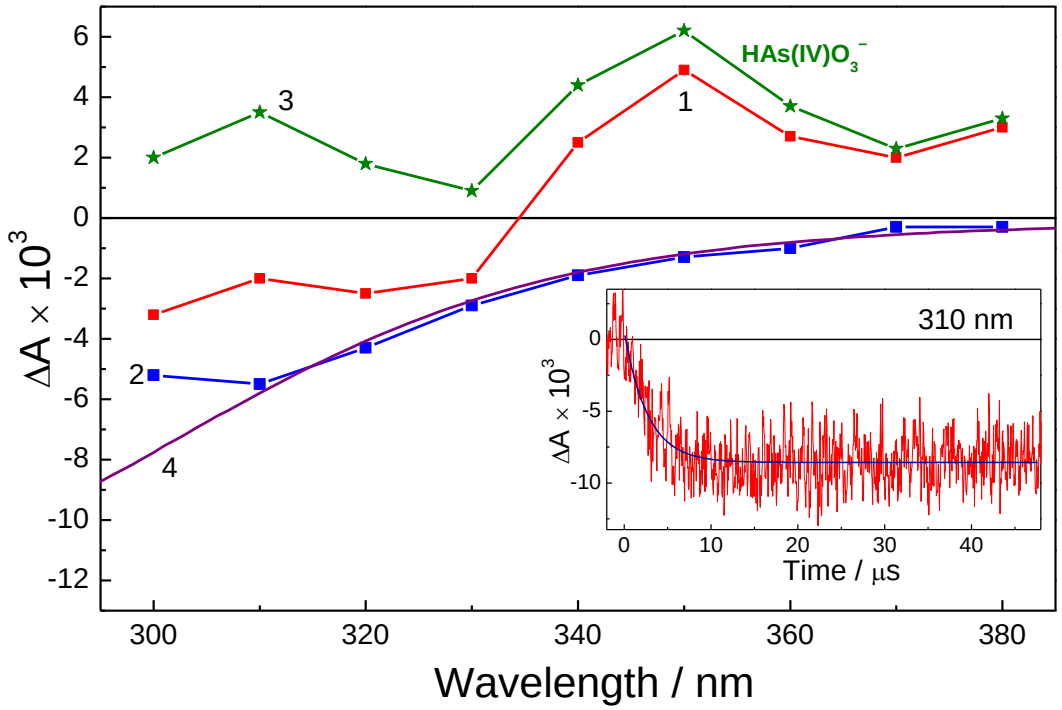

Fig. 4 Flash photolysis (266 nm) of the Fe(III)–As(III) system at pH 3. Δ*A* is the change in optical density. $[Fe(III)(ClO_4)_3]$ = 0.34 mM, [As(III)] = 17 mM, excitation energy = 4.6 mJ/pulse. (1, 2) Transient spectra obtained at 0.05 and 48 μs after excitation, respectively. (3) Difference between spectra in (1) and (2) corresponding to the spectrum of $HAs(IV)O_3^-$.[39] (4) Inverted absorption spectrum of the $[Fe(III)(H_2AsO_3)_2]^+$ complex. Inset: kinetic curve at 310 nm and the best monoexponential fit with a time constant of 3 μs.

Flash excitation of the Fe(III)–As(III) complex led to the appearance of a transient absorption with a maximum at 350 nm (Fig. 4). This transient signal is assumed to arise from $HAs(IV)O_3^-$, formed by electron

transfer from the ligand to iron (reaction 6), based on a comparison with the known absorption spectrum of $HAs(IV)O_3^-$.[39] The lifetime of the latter species was about 3 μs under the experimental conditions used (Fig. 4).

After the disappearance of the initial transient signal, constant bleaching corresponding to decay of the initial complex was observed (Fig. 4, curve 2). The amplitude of bleaching at 310 nm measured at times < 50 μs after excitation exhibited a linear dependence on the laser pulse intensity. This allowed us to estimate the quantum yield of $[Fe(H_2AsO_3)_2]^+$ complex photolysis (0.023) by using a known value of the molar absorption coefficient (2400 M^{-1} cm^{-1} at 310 nm). The absorption coefficient of the complex at 310 nm was obtained by the same procedure as for the absorption coefficient at 260 nm. The quantum yield of $[Fe(H_2AsO_3)_2]^+$ complex photolysis was close to that of Fe(II) photoproduction at 266 nm. The difference between these values could be explained by reactions (11–13) occurring on timescales longer than 50 μs. The quantum yield of the $[Fe(H_2AsO_3)_2]^+$ complex photolysis in acid aqueous solution was similar to that of the As(III)–CFH complex in the CFH system (ca. 0.01).[19]

On the basis of aforesaid findings, we propose the following general mechanism of $[Fe(H_2AsO_3)_2]^+$ complex photolysis at pH 3:

$$[Fe(H_2AsO_3)_2]^+ + h\nu \rightarrow [Fe(II)\text{-}As(IV)] \rightarrow Fe(II) + HAs(IV)O_3^- + H_3AsO_3 \quad (6)$$

$$HAs(IV)O_3^- + O_2 + H_2O \rightarrow H_2As(V)O_4^- + HO_2^\bullet,\ k_8 = 10^9\ M^{-1}\ s^{-1}\ [39] \quad (7)$$

$$HAs(IV)O_3^- + Fe(III) + H_2O \rightarrow Fe(II) + H_2As(V)O_4^- + H^+ \quad (8)$$

$$HAs(IV)O_3^- + HO_2^\bullet + 2H^+ \rightarrow H_2As(V)O_4^- + H_2O \quad (9)$$

$$HO_2^\bullet + HO_2^\bullet \rightarrow O_2 + H_2O_2,\ k_{11} = 8.3 \times 10^5\ M^{-1}\ s^{-1}\ [37] \quad (10)$$

$$Fe(II) + HO_2^\bullet + H^+ \rightarrow Fe(III) + H_2O_2,\ k_{12} = 1.2 \times 10^6\ M^{-1}\ s^{-1}\ [40] \quad (11)$$

$$Fe(III) + HO_2^\bullet \rightarrow Fe(II) + O_2 + H^+,\ k_{13} = 2 \times 10^3\ M^{-1}\ s^{-1}\ [40] \quad (12)$$

$$Fe(II) + H_2O_2 + H^+ \rightarrow Fe(III) + {}^{\bullet}OH + H_2O,\ k_{14} = 63\ M^{-1}\ s^{-1}\ [40] \quad (13)$$

$$^{\bullet}OH + H_3AsO_3 \rightarrow HAs(IV)O_3^- + H_2O + H^+,\ k_{15} = 8.5 \times 10^9\ M^{-1}\ s^{-1}\ [39] \quad (14)$$

$$Fe(III) + As(V) \rightarrow Fe(III)–As(V)\ (insoluble) \quad (15)$$

where k_n are the rate constants of the reactions, with n being the number of the corresponding equation. According to this mechanism, the first photochemical step is intersphere oxidation of the ligand, which leads to the formation of an unstable [Fe(II)–As(IV)] complex. This species dissociates at times shorter than 50 ns with the formation of Fe(II) and As(IV) (reaction 6). This assumption is based on the detection of non-coordinated $HAs(IV)O_3^-$ immediately after excitation of $[Fe(H_2AsO_3)_2]^+$ and on the fact that elimination of an $^{\bullet}OH$ radical upon excitation of the $FeOH^{2+}$ complex occurs in less than 50 ns.[41] Initially formed As(IV) is mainly oxidized by dissolved oxygen and Fe(III) ions to As(V) in reactions (8, 9), which determine the lifetime of $HAs(IV)O_3^-$ (ca. 3 μs). Additional oxidation of Fe(II) in Fenton-like reactions (11, 13) leads to the generation of ROS, which can participate in further oxidation of As(III) and As(IV) (Eqs. (9) and (14)) on a longer time scale.

In the final step, colloidal $FeAsO_4$ is formed (Eq. (15)). To test this hypothesis, colloids obtained after photolysis and the product in solution obtained by preparation of the Fe(III)–As(V) complex were analyzed for particle size and by UV/visible (UV/Vis) spectrophotometry. Fig. S5 shows photographs of the white colloids that formed by direct mixing of Fe(III) and As(V) (A) and during photolysis of the Fe(III)–As(III) complex (B) at pH 3. Both colloids were stable and did not precipitate. Fig. S6 shows the particle size distributions of the colloids. The size of colloidal particles formed after photolysis was 5–54 μm, whereas the particles of the Fe(III)–As(V) complex were of size 3–48 μm. We could not separate the colloidal particles from the solution by filtration or centrifugation. However, the UV/Vis spectra of the colloids in Fig. S7 feature similar light absorption bands in the range 250–600 nm, confirming $FeAsO_4$ formation during

photolysis of the Fe(III)–As(III) complex.

Photochemistry of the aqueous Fe(III)-As(III) system at low As(III) concentration: $Fe(III)OH^{2+}$ photolysis and mechanism of As(V) formation

At low arsenite concentrations, the Fe(III)–As(III) system exhibits interesting photochemistry without evident sedimentation and turbidity. At 1 mM As(III), 0.34 mM Fe(III), and pH 3, less than 10% of the Fe(III) forms complexes with As(III) (Fig. 1). At pH 3, most Fe(III) (ca. 80%) exists as $FeOH^{2+}$, which undergoes photolysis to produce an $^{\bullet}OH$ radical (Eq. (16)).[41]

$$FeOH^{2+} + h\nu \rightarrow {}^{\bullet}OH + Fe(II) \qquad (16)$$

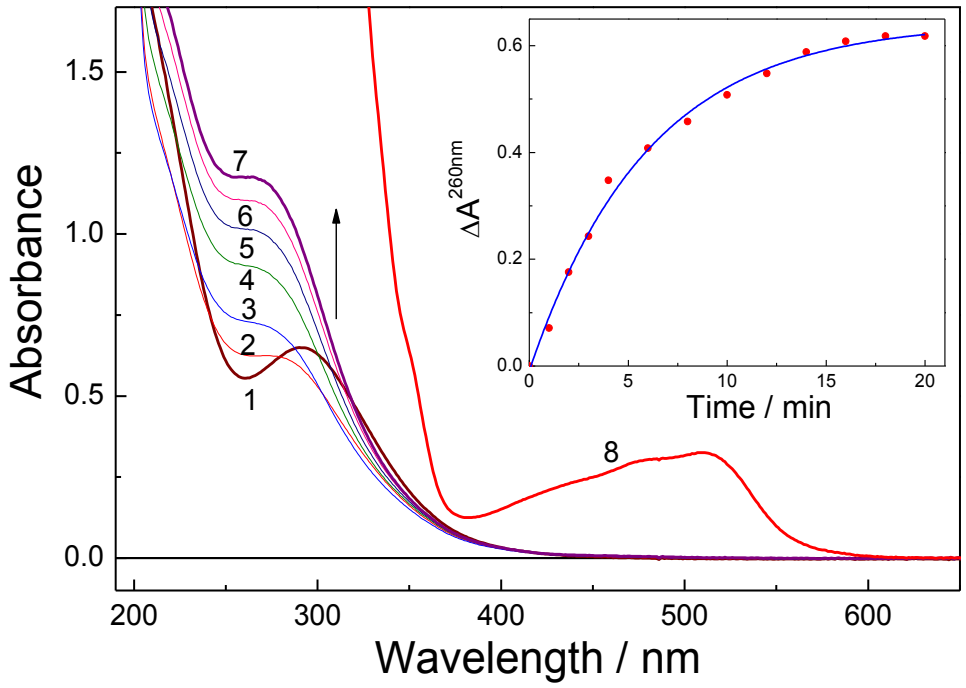

Fig. 5 Steady-state photolysis (308 nm) of the $FeOH^{2+}$–As(III) system at pH 3. Experimental conditions: $[Fe(III)(ClO_4)_3]$ = 0.34 mM, [As(III)] = 1.1 mM, sample volume 2 mL, incident light intensity = 1.4×10^{16} quanta/s or 0.56 mM/min. (1–7) Spectra after 0 (1), 1 (2), 2 (3), 4 (4), 8 (5), 12 (6), and 20 min (7) of irradiation. (8) Spectrum of the solution irradiated for 20 min after the addition of *o*-phenanthroline. Inset: changes in optical density at 260 nm during irradiation.

During photolysis at 308 nm (Fig. 5) or 266 nm (Fig. S8), Fe(II) and an unknown photoproduct showing absorbance at 260 nm were formed. We assume the photoproduct to be an unidentified Fe(III) complex, since inorganic Fe(II) complexes exhibit low absorption in the UV region.[25,42] Identification of the photoproduct will be the subject of further work.

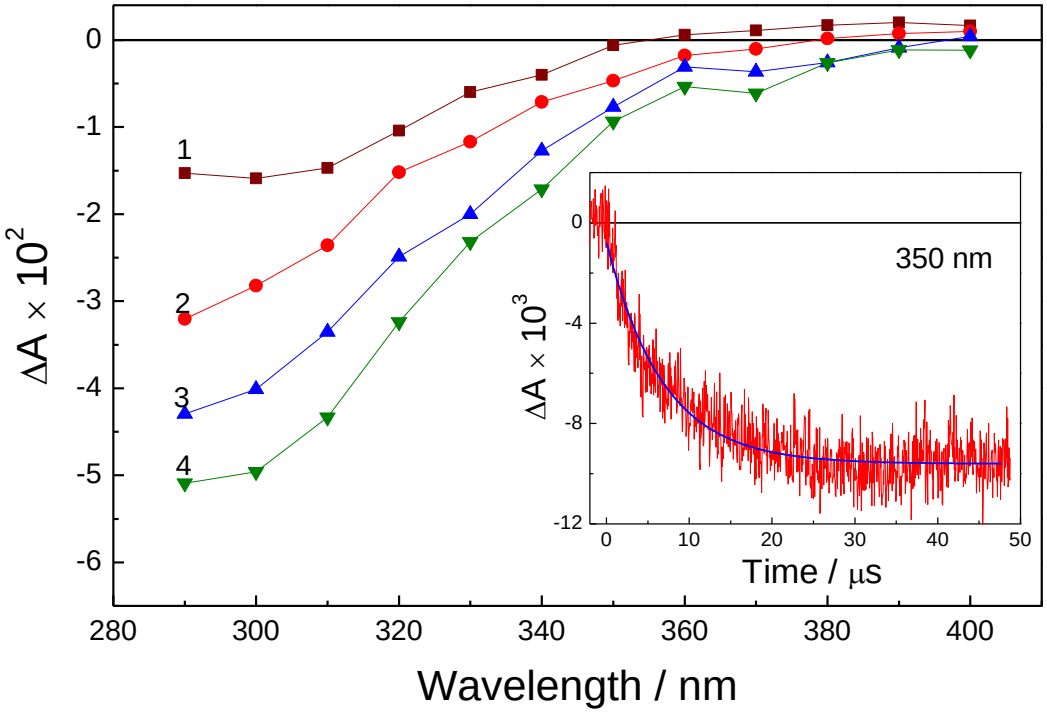

Fig. 6 Flash photolysis (266 nm) of the $FeOH^{2+}$–As(III) system at pH 3 in argon-saturated solution. Δ*A* is the change in optical density. Experimental conditions: [Fe(III)(ClO_4)$_3$] = 0.34 mM, As(III) = 0.5 mM. (1–4) Transient spectra at 0.2 (1), 2.8 (2), 10 (3), and 48 μs (4) after excitation. Inset: kinetic curve at 350 nm and the best monoexponential fit with a time constant of 7 μs.

Excitation at 266 nm is favorable for the formation of Fe(II), whereas excitation at 308 nm leads to a greater photoproduct yield. We tentatively assume that the photoproduct is photoactive and that its excitation at 266 nm leads to the formation of additional Fe(II).

Flash excitation of $FeOH^{2+}$ in the presence of As(III) led to the formation of a transient absorption signal

superimposed with bleaching because of the disappearance of the absorption of the complex (Fig. 6). This signal can be assigned to As(IV)$(OH)_4$,[39] formed in a reaction with As(III) ions:

$^{\bullet}OH + H_3AsO_3 = As(IV)(OH)_4$, $k = 8.5 \times 10^9$ M^{-1} s^{-1} [33] (17)

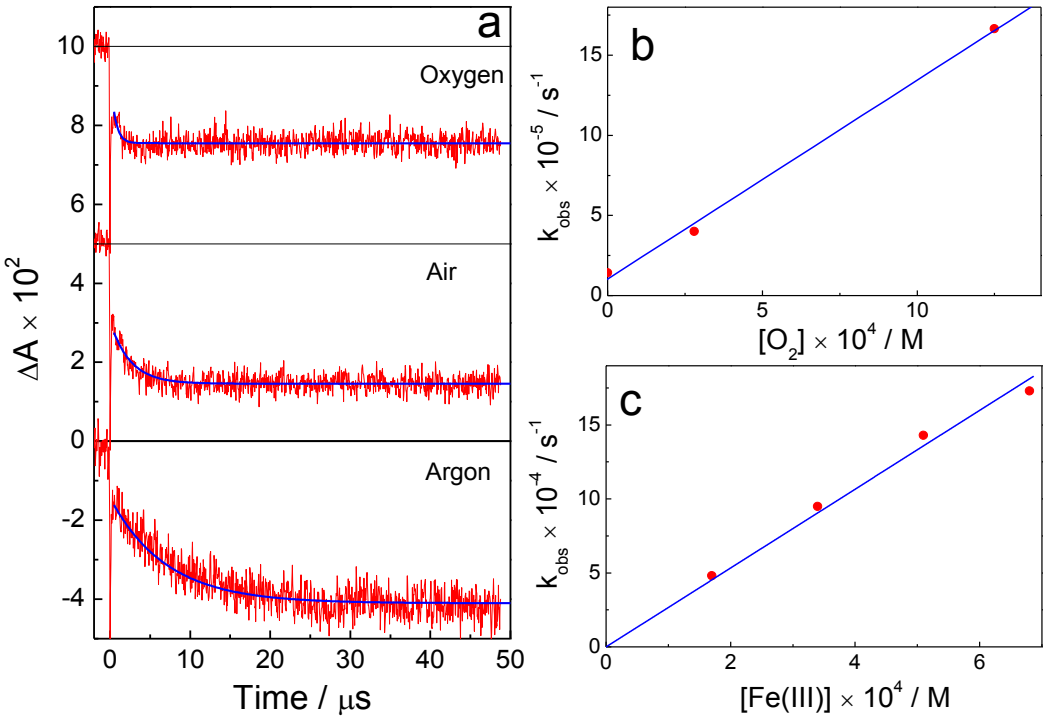

Fig. 7 Flash photolysis (266 nm) of the $FeOH^{2+}$–As(III) system at pH 3. ΔA is the change in optical density. (a) Kinetic curves at 310 nm in solutions with various oxygen concentrations. Smooth curves are the best monoexponential fits obtained by using Eq. (20). Experimental conditions: [Fe(III)$(ClO_4)_3$] = 0.34 mM, As(III) = 0.5 mM. (b) Dependence of the observed rate constant (k_{obs}) on the concentration of dissolved oxygen. Experimental conditions: [Fe(III)$(ClO_4)_3$] = 0.34 mM, As(III) = 0.5 mM. (c) Dependence of k_{obs} on the concentration of total Fe(III). Experimental conditions: argon-saturated solution, As(III) = 0.5 mM.

As(IV)$(OH)_4$ decay depends on the oxygen and Fe(III) concentrations (Fig. 7a–c):

$As(IV)(OH)_4 + O_2 \rightarrow H_2As(V)O_4^- + HO_2^{\bullet} + H^+$, $k_{18} = 1.3 \pm 0.1 \times 10^9$ M^{-1} s^{-1} (our LFP data) (18)

$As(IV)(OH)_4 + Fe(III) \rightarrow H_2As(V)O_4^- + Fe(II) + 2H^+$, $k_{19} = 2.7 \pm 0.1 \times 10^8$ M^{-1} s^{-1} (our LFP data) (19)

Reactions (18) and (19) compete with each other, as shown by the kinetic curves in Fig. 7a. An increase in oxygen content in solution leads to a decrease in the lifetime of As(IV)$(OH)_4$ and to additional bleaching at 310 nm caused by reaction (19). Treatment of a set of kinetic curves at 310 nm obtained at different oxygen and Fe(III) contents by Eq. (20) allowed us to determine the rate constants of reactions (18) and (19) from the linear dependences of the observed rate constants (k_{obs}) on the oxygen and Fe(III) concentrations (Fig. 7b and c):

$$\Delta A(t) = A_0 \exp(-k_{obs}t),\ k_{obs} = k_{18}[O_2] + k_{19}[\text{Fe(III)}] \quad (20)$$

where ΔA(t) is the change in optical density, and A_0 is the initial optical density. The value of k_{18} agrees well with that obtained by Klaning et al. ($k = 1.4 \times 10^9\ M^{-1}\ s^{-1}$).[39] Thus, the LFP experiments confirmed the oxidation of As(III) by photogenerated $^{\bullet}OH$ radicals with the formation of active As(IV) species. These species in turn undergo oxidation to As(V) through reactions (18) and (19). The final reaction step should be the same as for solutions with high As(III) concentration (reaction (15)).

Photolysis of the solid product of the Fe(III)–As(III) complex

As(III) photooxidation during photolysis of the solid product of the Fe(III)–As(III) complex was observed, as shown in Fig. 8. After 50 min, the remaining As(III) in the sample had decreased to almost 75% of the initial value. Because of light attenuation by the surface of the solid product, light cannot penetrate to the interior of the product. The As(III) was not further oxidized after 50 min. The energy of UV-C irradiation in terms of wavelength and intensity is much lower than that of the X-rays used for XPS analysis. The oxidation efficiency of As(III) (25%) under UV-C irradiation was much lower than that associated with XPS analysis (82.4%). This result implies that the Fe(III)–As(III) complex is sensitive to UV-C light and that As(III) is prone to oxidation to As(V) through LMCT, even in the solid phase.

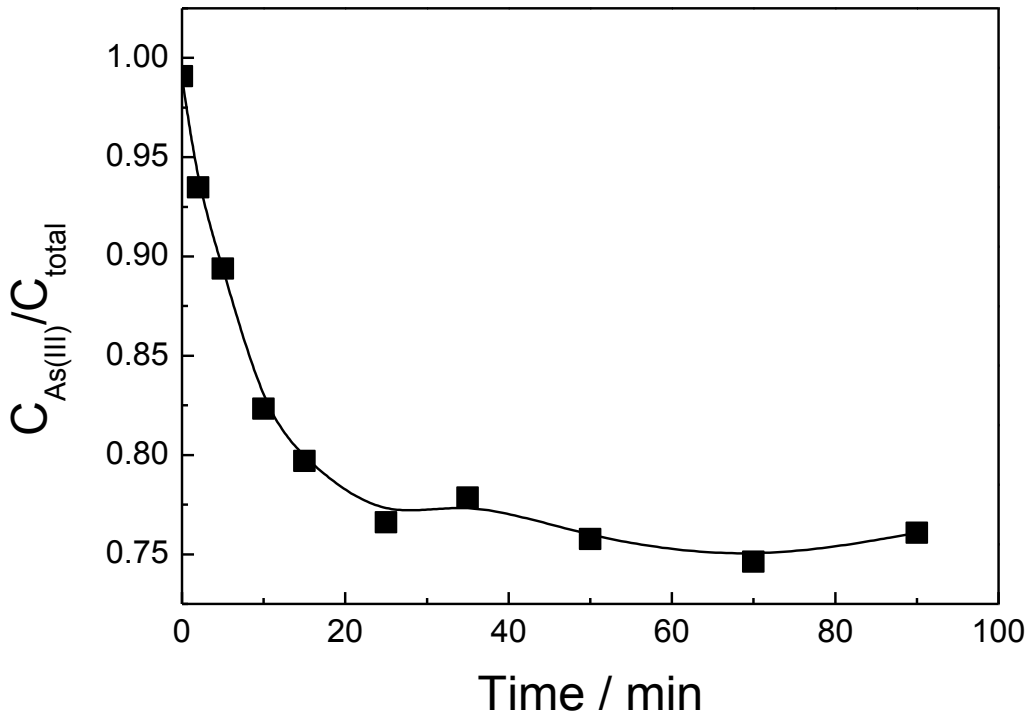

Fig. 8 Steady-state photolysis of the solid Fe(III)–As(III) complex under UV-C irradiation (dominant wavelength 254 nm). $C_{As(III)}/C_{total}$ is the proportion of As(III) in the total arsenic. The complex was the same as that used in the XPS and XRD measurements; its Fe/As molar ratio was 1:0.92.

Conclusions

At high As(III)/Fe(III) ratio in solution at pH 3, an Fe(III)–As(III) complex forms as $[Fe(H_2AsO_3)_2]^+$. This complex undergoes photolysis in acid solution with an Fe(II) production quantum yield of about 0.012. Formation and photolysis of the Fe(III)–As(III) (Fe/As = 1:0.92) complex in the solid state were also observed. As(III) in solution is oxidized to As(IV) through an LMCT mechanism and then to As(V) mainly by the action of dissolved oxygen. At lower As(III)/Fe(III) ratio, As(III) photooxidation in acidic solution occurs through indirect oxidation by the hydroxyl radical produced by photolysis of $Fe(OH)^{2+}$. These two mechanisms of As(III) photooxidation in aqueous solutions could account for rapid oxidative transformation of As(III) to As(V) in acid mine drainage exposed to sunlight. The relative contributions of these two

mechanisms depend on the As(III)/Fe(III) ratio. This work demonstrates that the complexation and photooxidation process of Fe(III)-As(III) complexes should be taken into account when studying the fate of arsenic in acidic water containing Fe(III).

Acknowledgements

The work was financially supported by Russian Foundation for Fundamental Research (grants 11-03-00268, 12-03-00482, 12-03-91153-GFEN), NSFC-RFBR grants (21211120159 and 21281220200) and National Natural Science Foundation of China (Grant Nos. 21077080, 21477090).

References

1 S. L. Wang and C. N. Mulligan, Natural attenuation processes for remediation of arsenic contaminated soils and groundwater, *J. Hazard. Mater.*, 2006, **138**(3), 459–470.

2 H. Cheng, Y. Hu, J. Luo, B. Xu and J. Zhao, Geochemical processes controlling fate and transport of arsenic in acid mine drainage (AMD) and natural systems, *J. Hazard. Mater.*, 2009, **165**, 13–26.

3 T. M. Clancy, K. F. Hayes and L. Raskin, Arsenic waste management: a critical review of testing and disposal of arsenic-bearing solid wastes generated during arsenic removal from drinking water, *Environ. Sci. Technol.*, 2013, **47**(19), 10799–10812.

4 T. J. Sorg, A. S. Chen and L. Wang, Arsenic species in drinking water wells in the USA with high arsenic concentrations, *Water Res.*, 2014, **48**, 156–169.

5 M. R. Lescano, C. S. Zalazar, A. E. Cassano and R. J. Brandi, Arsenic (III) oxidation of water applying a combination of hydrogen peroxideand UVC radiation, *Photochem. Photobiol. Sci.*, 2011, **10**, 1797–1803.

6 S. H. Yoon, J. H. Lee, S. E. Oh and J. E. Yang, Photochemical oxidation of As(III) by vacuum-UV lamp irradiation, *Water Res.*, 2008, **42**(13), 3455–3463.

7 R. Jungho, M. S. Dami án, K. Dong-Hyo, Y. Jiman and C. Wonyong, Photooxidation of arsenite under 254 nm irradiation with a quantum yield higher than unity, *Environ. Sci. Technol.*, 2013, **47**(16), 9381–9387.

8 T. Wang, W. C. Yang, T. T. Song, C. F. Li, L. Y. Zhang, H. Y. Wang and L. Y. Chai, Cu doped Fe_3O_4 magnetic adsorbent for arsenic: synthesis, property, and sorption application, *RSC Adv.*, 2015, **15**, 50011-50018.

9 S. Tresintsi, K. Simeonidis, G. Vourlias, G. Stavropoulos and M. Mitrakas, Kilogram-scale synthesis of iron oxy-hydroxides with improved arsenic removal capacity: Study of Fe(II) oxidation–precipitation parameters, *Water Res.*, 2012, **46**(16), 5255–5267.

10 S. J. Hug, L. Canonica, M. Wegelin, D. Gechter and U. von Gunten, Solar oxidation and removal of arsenic at circumneutral pH in iron containing waters, *Environ. Sci. Technol.*, 2001, **35**, 2114–2121.

11 S. J. Hug and O. Leupin, Iron-catalyzed oxidation of arsenic (III) by oxygen and by hydrogen peroxide: pH-dependent formation of oxidants in the Fenton reaction, *Environ. Sci. Technol.*, 2003, **37**, 2734–2742.

12 M. T. Emett and G. H. Khoe, Photochemical oxidation of arsenic by oxygen and iron in acidic solutions, *Water Res.*, 2001, **35**, 649–656.

13 B. D. Kocar and W. P. Inskeep, Photochemical oxidation of As(III) in ferrioxalate solutions, *Environ. Sci. Technol.*, 2003, **37**, 1581–1588.

14 N. Bhandari, R. J. Reeder and D. R. Strongin, Photoinduced oxidation of arsenite to arsenate on ferrihydrite, *Environ. Sci. Technol.*, 2011, **45**, 2783–2789.

15 N. Bhandari, R. J. Reeder and D. R. Strongin, Photoinduced oxidation of arsenite to arsenate in the presence of goethite. *Environ. Sci. Technol.*, 2012, **46**, 8044–8051.

16 Y. J. Wang, J. Xu, Y. Zhao, L. Zhang, M. Xiao and F. Wu, Photooxidation of arsenite by natural goethite

414 in suspended solution, *Environ. Sci. Pollut. Res.*, 2013, **20**, 31–38.

415 17 Y. J. Wang, J. Xu, J. Li and F. Wu, Natural montmorillonite induced photooxidation of As (III) in aqueous

416 suspensions: Roles and sources of hydroxyl and hydroperoxyl/superoxide radicals, *J. Hazard. Mater.*,

417 2013, **260**, 255–262.

418 18 G. Liu, A. Fernandez and Y. Cai, Complexation of arsenite with humic acid in the presence of ferric iron,

419 *Environ. Sci. Technol.*, 2011, **45**, 3210-3216.

420 19 J. Xu, J. J. Li, F. Wu and Y. Zhang, Rapid Photooxidation of As(III) through surface complexation with

421 nascent colloidal ferric hydroxide, *Environ. Sci. Technol.*, 2014, **48**, 272–278.

422 20 R. Woods, I. M. Kolthoff and E. J. Meehan, Arsenic(IV) as an intermediate in the induced oxidation of

423 arsenic(III) by the iron(II)-persulfate reaction and the photoreduction of iron(III). I. Absence of oxygen,

424 *J. Am. Chem. Soc*., 1963, **85**, 2385–2390.

425 21 R. Woods, I. M. Kolthoff and E. J. Meehan, Arsenic(IV) as an intermediate in the induced oxidation of

426 arsenic(III) by the iron(II)-persulfate reaction and the photoreduction of Iron(III). II. Presence of oxygen,

427 *J. Am. Chem. Soc*., 1963, **85**, 3334–3337.

428 22 R. Woods, I. M. Kolthoff and E. J. Meehan, Arsenic (IV) as an intermediate in the induced oxidation of

429 arsenic (III) by the iron (II)-hydrogen peroxide reaction, *J. Am. Chem. Soc.* 1964, **86**, 1698–1700.

430 23 A. J. Bednar, J. R. Garbarino, J. F. Ranville and T. R. Wildeman, Effects of iron on arsenic speciation and

431 redox chemistry in acid mine water, *J. Geochem. Explor.*, 2005, **85**, 55–62.

432 24 I. P. Pozdnyakov, V. F. Plyusnin, V. P. Grivin, D. Y. Vorobyev, N. M. Bazhin and E. Vauthey, Photolysis of

433 sulfosalicylic acid in aqueous solutions over a wide pH range, *J. Photochem. Photobiol. A: Chem.*, 2006,

434 **181**, 37–43.

435 25 C. Weller, S. Horn, H. Herrmann, Effects of Fe(III)-concentration, speciation, excitation-wavelength and

light intensity on the quantum yield of iron(III)-oxalato complex photolysis, *J. Photochem. Photobiol. A: Chem.* 2013, **255**, 41–49.

26. A. E. Hargrove, Z. Zhong, J. L. Sessler, E. V. Anslyn, Algorithms for the determination of binding constants and enantiomeric excess in complex host: guest equilibria using optical measurements, *New J. Chem.*, 2010, **34**, 348–354.

27 C. Ren, H. Peng, W. Y. Huang, Y. J. Wang and F. Wu, Speciation of inorganic As(V)/As(III) in water and soil by hydride generation-atomic fluorescence spectrometry, *Fresen. Environ. Bull.*, 2011, **20**, 1069–1074.

28 H. J. Benkenberg and P. Warneck, Photodecomposition of iron(III) hydroxo and sulfato complexes in aqueous solution: Wavelength dependence of OH and SO_4^- quantum yields, *J. Phys. Chem.*, 1995, **99**, 5214–5221.

29 F. Al-Sogair , H. M. Marafie , N. M. Shuaib , H. Ben Youngo, M. S. El-Ezaby, Interaction of phosphate with iron(III) in acidic medium, equilibrium and kinetic studies, *J. Coord. Chem.*, 2002, **55**, 1097.

30 G. Lente, I. Fâbián, Ligand substitution kinetics of the iron(III) hydroxo dimer with simple inorganic ligands, *Inorg. Chem.*, 2002, **41**, 1306–1314.

31 W. Feng, D. Nansheng, Photochemistry of hydrolytic iron(III) species and photoinduced degradation of organic compounds. A minireview, *Chemosphere*, 2000, **41**, 1137–1147.

32 Y. F. Jia, L. Xu, X. Wang and G. P. Demopoulos, Infrared spectroscopic and X-ray diffraction characterization of the nature of adsorbed arsenate on ferrihydrite, *Geochim. Cosmochim. Ac.*, 2007, **71**, 1643–1654.

33 G. Leonhardt, A. Berndtsson, J. Hedman, M. Klasson, R. Nilsson and C. Nordling, ESCA studies of some $A^{III}B^{v}$ compounds with Ga and As, *Phys. Status Solidi B.*, 1973, **60**, 241–248.

458 34 H. Nesbitt, G. Canning and G. Bancroft, XPS study of reductive dissolution of 7 Å-birnessite by H_3AsO_3,
459 with constraints on reaction mechanism, *Geochim. Cosmochim. Ac.*, 1998, **62**, 2097–2110.
460 35 W. J. Stec, W. E. Morgan, R. G. Albridge and J. R. Van Wazer, Measured binding energy shifts of "3p" and
461 "3d" electrons in arsenic compound, *Inorg. Chem.*, 1972, 11, 219–225.
462 36 M. Ding, B. H. W. S. de Jong, S. J. Roosendaal and A. Vredenberg, XPS studies on the electronic structure
463 of bonding between solid and solutes: adsorption of arsenate, chromate, phosphate, Pb^{2+}, and Zn^{2+} ions
464 on amorphous black ferric oxyhydroxide, *Geochim. Cosmochim. Ac.*, 2000, **64**, 1209–1219.
465 37 B. M. Daniels and J. Weiss, Chemical action of ionising radiations in solution. Part XXII. The radiation
466 chemistry of arsenite solutions: the action of X-rays (200 kv) on aqueous solutions of arsenite, *J. Chem.*
467 *Soc.*, 1958, 2467–2471.
468 38 J. Sima and J. Makanova, Photochemistry of iron(III) complexes, *Coord. Chem. Rev.*, 1997, **160**,
469 161–189.
470 39 U. K. Kläning, B. H. J. Bielski and K. Sehested, Arsenic(IV). A pulse-radiolysis study, *Inorg. Chem.*, 1989,
471 **28**, 2717–2724.
472 40 S. Barreca, J. J. V. Colmenares, A. Pace, S. Orecchio and C. Pulgarin, Neutral solar photo-Fenton
473 degradation of 4-nitrophenol on iron-enriched hybrid montmorillonite-alginate beads (Fe-MABs), *J.*
474 *Photochem. Photobiol. A: Chem.*, 2014, **282**, 33–40.
475 41 I. P. Pozdnyakov, E. M. Glebov, V. F. Plyusnin, V. P. Grivin, Yu. V. Ivanov, N. M. Bazhin and D. Yu.
476 Vorobjev, Mechanism of $Fe(OH)^{2+}$(aq) Photolysis in aqueous solution, *Pure Appl. Chem.*, 2000, **72**,
477 2187–2197.
478 42 J. Jortnor and G. J. Stein, The photochemical evolution of hydrogen from aquesou solution of ferrous ions.
479 Part I. The reaction mechanism at low pH, *Phys. Chem.*, 1962, **66**, 1258–1264.

Graphical Abstract

Fe(III)–As(III) complex is characterized by UV/Vis spectra and its laser flash photolysis occurring via ligand-to-metal charge transfer results in the intermediate of Fe(II)–As(IV).

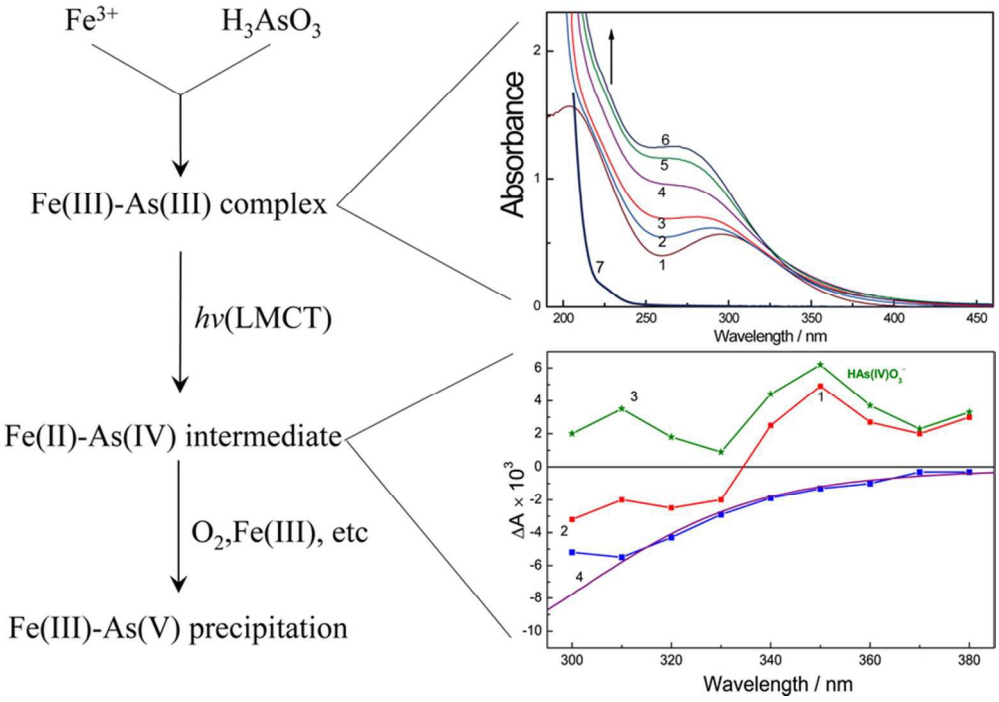

39x28mm (600 x 600 DPI)